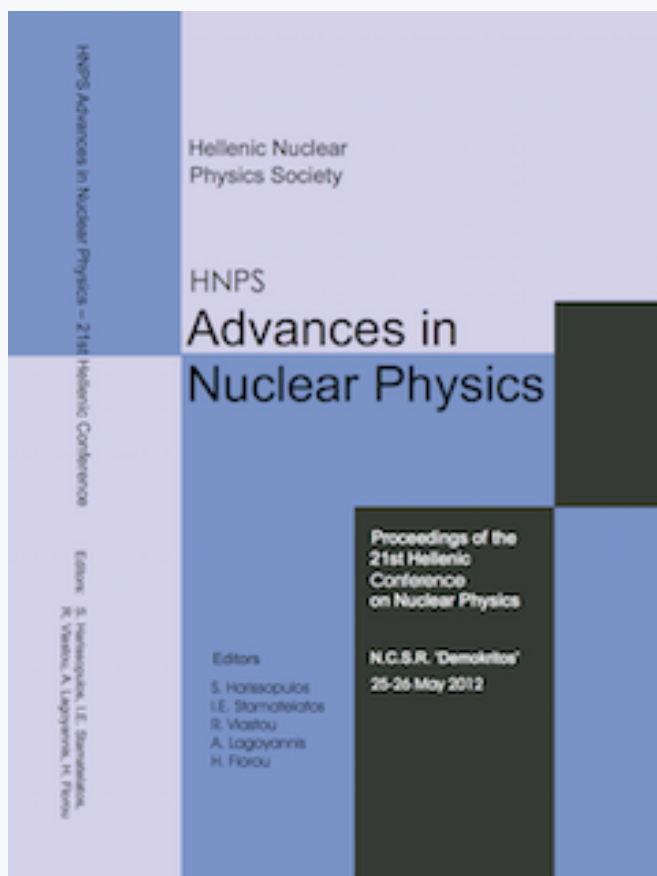


## HNPS Advances in Nuclear Physics

Vol 20 (2012)

HNPS2012



### Characterization of actinide targets for fission cross section measurements

*M. Diakaki, R. Vlastou, M. Kokkoris, D. Karadimos, A. Lagoyannis, M. Axiotis, K. Ioannides, K. Stamoulis*

doi: [10.12681/hnps.2491](https://doi.org/10.12681/hnps.2491)

#### To cite this article:

Diakaki, M., Vlastou, R., Kokkoris, M., Karadimos, D., Lagoyannis, A., Axiotis, M., Ioannides, K., & Stamoulis, K. (2012). Characterization of actinide targets for fission cross section measurements. *HNPS Advances in Nuclear Physics*, 20, 81–88. <https://doi.org/10.12681/hnps.2491>

# Characterization of actinide targets for fission cross section measurements

M. Diakaki<sup>a</sup>, R. Vlastou<sup>a</sup>, M. Kokkoris<sup>a</sup>, D. Karadimos<sup>a</sup>,  
A.Lagoyannis<sup>b</sup>, M. Axiotis<sup>b</sup>, K. Ioannides<sup>c</sup>, K. Stamoulis<sup>c</sup>

<sup>a</sup>*Department of Physics, National Technical University of Athens, 157 80 Athens, Greece.*

<sup>b</sup>*Institute of Nuclear Physics, N.C.S.R. "Demokritos", GR-15310 Aghia Paraskevi, Attiki, Greece.*

<sup>c</sup>*Department of Physics, University of Ioannina, Ioannina 451 10, Greece.*

---

## Abstract

In this work the characterization of thin actinide targets ( $^{237}\text{Np}$ ,  $^{238}\text{U}$ ,  $^{235}\text{U}$ ), manufactured for measurements of fission cross section, will be presented. The determination of the mass of the actinide content of each target has been performed via alpha spectrometry, utilizing two SSB detectors, with  $50\text{mm}^2$  and  $3000\text{mm}^2$  active surface, in order to combine good resolution and good statistics respectively and obtain a smaller error in the final mass result. The impurities of the targets were quantitatively estimated with the same technique. The homogeneity of the samples was examined with two independent methods. Firstly, RBS measurements were performed using a proton beam of 2 MeV, provided by the 5.5 MV Tandem Van de Graaff accelerator of the N.C.S.R. "Demokritos". The thickness of each target was quantitatively estimated at various points. Secondly, CR-39 plastic track detectors were used to measure the alpha tracks from the surface of the targets and provide an image of the activity of the surface.

---

## 1 Introduction

The present work is in the context of a wider project that concerns the measurement of the cross section of the  $^{237}\text{Np}(n,f)$  reaction. This measurement has already been performed at the n\_TOF facility at CERN with use of a white neutron beam and the FIC ionization chamber and a new measurement of this cross section is being planned in the near future using monoenergetic neutron beams at the Institute of Nuclear Physics at N.C.S.R. "Demokritos", implementing a new MicroMegas detector constructed at CERN for these measurements, in the context of the n\_TOF collaboration.

The experimental determination of accurate cross section data requires the knowledge of the number of nuclei that the target contains, both for the target of interest and the reference target, with high precision. It is also important to know the distribution of the nuclei on the surface of the target, especially when the incident beam is inhomogeneous as far as its energy and/or spatial distribution is concerned. The actinide targets used,  $^{237}\text{Np}$  and the reference targets  $^{238}\text{U}$  and  $^{235}\text{U}$  are thin disks of actinide oxides ( $\text{NpO}_2$  and  $\text{U}_3\text{O}_8$ ), deposited on  $100\ \mu\text{m}$  Al backing via the painting technique. They were provided by the Institute of Physics and Power Engineering, Obninsk, and the Joint Institute of Nuclear Research, Dubna. The measurement of the mass of each target and of their impurities along with the determination of their homogeneity was the goal of the present work.

## 2 Total mass measurements

The actinide targets under study are purely alpha emitters. The mass  $m$  of the actinide content is the ratio of the alpha activity at  $4\pi$  ( $A_{4\pi}$ ) to the corresponding specific activity ( $A_{/mg}$ ):  $m = \frac{A_{4\pi}}{A_{/mg}}$ . The latter is a characteristic value for each isotope and for long half lives, as in this case, it only depends on the half life ( $T_{1/2}$ ) and mass number ( $A$ ):  $A_{/mg} = \frac{\ln(2)N_A}{1000T_{1/2}A}$ , where  $N_A$  is the Avogadro constant. The activity at  $4\pi$  can't be directly measured, but can be determined by measuring the activity in a solid angle  $\Omega$  subtended by a detector ( $A_\Omega$ ). Since the alpha emission is isotropic, the activity at  $4\pi$  ( $A_{4\pi}$ ) is given by:  $A_{4\pi} = \frac{4\pi A_\Omega}{\Omega}$ . Thus, the mass value  $m$  for a given isotope is given by eq. 1.

$$m = \frac{4\pi A_\Omega}{\Omega A_{/mg}}, \quad (1)$$

In the present work, the activity of each target was measured with two SSB detectors with different active surfaces. A small detector with  $50\ \text{mm}^2$  was used in order to obtain good resolution, whereas a big detector with  $3000\ \text{mm}^2$  was used in order to increase statistics. A special holder for the targets and the detectors has been made in order to assure that a) the surface of both detectors would be at the same distance from the targets, b) the surface of the detectors would be coaxial to the targets and c) there would be a repetitivity of the geometrical conditions among all the targets measured. Tantalum masks were put in front of both detectors in order to avoid edge effects, the radius of which was carefully chosen in order to attain the highest possible acceptance while avoiding shadow effects (i.e. alphas that pass through the mask but don't enter the active surface of the detector). Thus, the active surface of each detector was determined from the mask hole, which could be more easily

and accurately measured. According to the geometrical measurements, the distance target-detector surface was  $d_{meas}=(15.8\pm 0.1)$  cm, the radius of the mask of the small and the big detector were  $r_{meas}=(0.350\pm 0.015)$  cm and  $R_{meas}=(2.902\pm 0.002)$  cm respectively.

The  $A_\Omega$  was estimated by integrating the total counts from the peak to the “noise threshold” because counts at lower energies than the “nominal” peak are due to energy losses in the target and scattering at the edges of the mask. Background measurements were used in order to estimate the channel from which the noise begins as well as possible background counts in the region of integration. The dead time in all the spectra used did not exceed 0.3%. The calibration of the spectra was done with use of a triple  $^{241}\text{Am}/^{239}\text{Pu}/^{244}\text{Cm}$  source.

For each setup, spectra from a calibrated  $^{241}\text{Am}$  source, well centered with respect to the detector axis, were taken in order to experimentally determine the  $\Omega$  subtended by the detectors from the source, namely the  $\Omega_{ss,exp}$  and  $\Omega_{sb,exp}$  for the small and big detector respectively. With use of the Gardner’s formalism [1] for disk-to-disk solid angle calculations an effective geometry was defined ( $d_{effective}$ ,  $r_{effective}$ ,  $R_{effective}$ ) in order to reproduce the  $\Omega_{ss,exp}$  and  $\Omega_{sb,exp}$  values, see Fig. 1. It turned out that a small change was needed to the  $d_{meas}$ ,  $r_{meas}$  and  $R_{meas}$  values (up to 1.1 %). With use of this effective geometry and the measured radius of the targets (see table 1) the  $\Omega_{bs}$  and  $\Omega_{bb}$  were defined with the Gardner’s formalism.

The uncertainties of the  $\Omega_{bs}$  and  $\Omega_{bb}$  are the quadratic sum of two factors: a) the uncertainty of the  $\Omega_{ss,exp}$  and  $\Omega_{sb,exp}$  values with which the effective distance and radius of the detectors were defined and b) the change in the calculated values when changing the geometrical parameters that were not fixed with the “effective geometry” within their experimental errors, for example the radius of the target. The final error did not exceed 1.9%.

As an extra check, the ratio  $\Omega_{bs}/\Omega_{bb}$  calculated with this method was compared to  $\Omega_{ss,exp}/\Omega_{sb,exp}$ . These two values should be equal within their errors since the activities cancel out. Furthermore, MCNPX [2] simulations of the setup showed that at this target-to-detector distance the correction needed at the sub-threshold counts between the source and the target spectra, due to scattering at the chamber and the holder, is negligible (of the order of 1 per thousand).

With the above method high accuracy mass values occurred (see table 1). For lower-activity targets, such as  $^{238}\text{U}$  and  $^{235}\text{U}$ , spectra from both detectors were used in order to extract two mass values and the final mass occurred from the weighted average value. For  $^{237}\text{Np}$  the intense pile-up effect precluded the use of the big detector spectra for the extraction of safe results, so the final mass

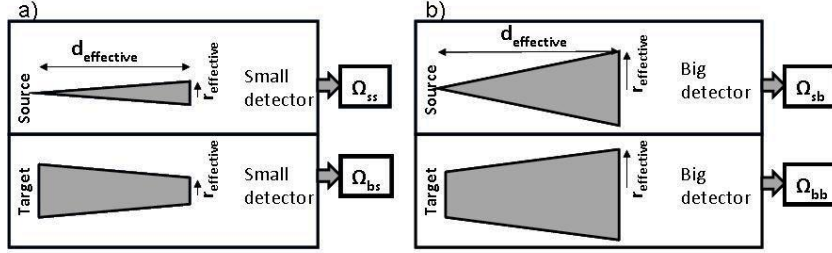


Fig. 1. Schematics of the effective geometry defined by experimental spectra from a calibrated  $^{241}\text{Am}$  source and the Gardner's formalism for disk-to-disk solid angle calculations for a) the small detector (active surface of 50 mm<sup>2</sup>) and b) the big detector (active surface of 3000 mm<sup>2</sup>).

Table 1  
Summary of the target properties

Target properties	$^{237}\text{Np}$	$^{238}\text{U}$	$^{235}\text{U}$
Oxide form	NpO <sub>2</sub>	U <sub>3</sub> O <sub>8</sub>	U <sub>3</sub> O <sub>8</sub>
Target Diameter (cm)	8	5.2	5.2
Half life (y)	$2.144 \cdot 10^6$	$4.468 \cdot 10^9$	$7.038 \cdot 10^8$
Specific Activity (Bq/mg)	$26031 \pm 85$	$12.44 \pm 0.01$	$79.98 \pm 0.06$
Mass values (mg)	$6.36 \pm 0.11$	$9.90 \pm 0.13$ (label:209) $9.03 \pm 0.12$ (label:210)	$4.96 \pm 0.06$
Contaminations (mg)	$^{241}\text{Am}(1.6 \cdot 10^{-5})$	-	$^{234}\text{U}(9 \cdot 10^{-5})$
Mean actinide surface concentration ( $10^{15}$ at/cm <sup>2</sup> )	$249 \pm 25$	$1112 \pm 95$ $1120 \pm 100$	$626 \pm 90$

value was derived only from the small detector. The contaminations of the targets were estimated with the same method and their amount turned out to be negligible (see table 1).

### 3 Thickness and homogeneity measurements

The actinide targets were examined as far as their thickness and homogeneity are concerned via the Rutherford Backscattering Spectrometry technique (RBS) at the external ion-beam setup of the 5.5 MV HV TN-11 Tandem accelerator of the Institute of Nuclear Physics at NCSR "Demokritos" [3]. The targets were mounted on a holder specially designed to provide the possibility to move perpendicularly with respect to the beam axis with an accuracy of 0.01 mm. The incident proton beam of 2 MeV traversed a 100 nm Si<sub>3</sub>N<sub>4</sub> window, then 3.8 mm of air and reached the surface of the actinide layer at

<sup>1</sup> The source was re-calibrated at the Institute for Reference Materials and Measurements (JRC-IRMM), right after the measurements, and the value of the activity was given with an uncertainty of 0.3%.

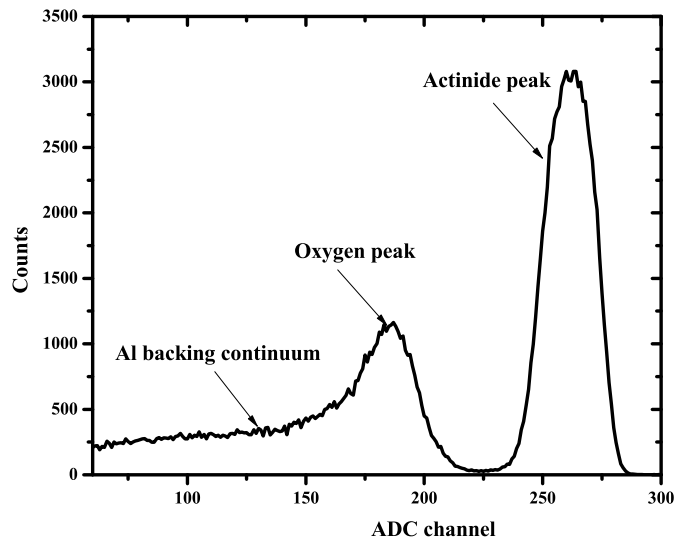


Fig. 2. Typical RBS spectrum from the central point on the surface of a  $^{238}\text{U}$  target. The protons scattered by the actinide content of the targets ("actinide peak") are well distinguished from those scattered at the aluminum backing ("Al backing continuum") and those scattered at the oxygen ("oxygen peak") from the actinide layer, the air and the aluminum backing of the targets.

the measurement point. The beam radius at the measurement point was approximately 1 mm. The elastically scattered protons traversed 28.5 mm of air and were detected by a silicon surface barrier detector, with a tantalum mask in order to avoid edge effects, at an angle of  $134^\circ$ . For each target 5-10 points were measured in order to check the homogeneity. A typical spectrum is shown in fig. 2.

Three ways were used in order to check the homogeneity of the targets. Firstly, a comparison of the ratio  $\frac{\text{ActinidePeakIntegralCounts}}{\text{AlbackingCounts}}$  among the different points was performed, keeping the same integration region among the points of the same target. This comparison is independent on the number of the impinging proton ions (namely  $Q$ ) and the solid angle subtended by the detector (namely  $\Omega$ ). Secondly, the FWHM of the actinide peak gives an estimation of the energy loss of the proton beam in the actinide layer and thus the thickness of the layer, so a comparison of the FWHM among the different points was also performed. Finally, the RBS spectrum occurring for each point was analyzed using SIMNRA v. 6.06 [4]. The actual experimental parameters (Ziegler-Biersack-Littmark stopping power data, Chu and Yang's straggling model, multiple scattering, choice of a small energy step for incoming and outgoing protons, beam divergence) were used as implemented in the code. This analysis includes a lot of free parameters in order to successfully describe the simulated experiment, such as the energy of the impinging proton beam, the calibration

of the RBS spectrum, the product  $Q\Omega$ , the detector resolution and the description of the absorber layer (which the scattered protons traverse until they reach the detector), the description of the target and its backing. In this work, according to SRIM calculations [5], the 2 MeV proton beam loses 5 keV at the  $\text{Si}_3\text{N}_4$  window and after 3.8 mm of air it reaches the measurement point with an energy of 1.931 MeV and energy spread of 6 keV. The calibration of the spectrum as well as the determination of the atomic concentration of the absorber layer (28.5 mm of air) were defined by the simulation of additional RBS spectra of thick Au, Ta and Al foils. The previously mentioned values were kept constant for all the measurement points. The  $Q\Omega$  product was defined by simulating the Al backing peak at each spectrum separately with an uncertainty less than 3%. For the  $^{237}\text{Np}$  target there was an additional difficulty due to the high alpha background under the whole spectrum. In this case the subtraction of the alpha background was done by using time-normalized beam-off spectra at each measurement point. For each point several values of detector resolution, actinide layer concentration and roughness were tried in order to reproduce the experimental spectrum. All gave similar values of actinide content and the average value was taken as the final result, and the final uncertainty did not exceed 3%. Thus, by comparing the actinide content among the different points on a target one can estimate the homogeneity.

The three methods gave consistent results within 10% and the targets were found to be homogeneous within approximately 15%. The mean value of the actinide content of all the points measured at each target is reported at table 1. The error reported in the table is the standard deviation of the mean value, the large value of which can be attributed to the small number of points. It has to be noted that the actinide surface concentration did not present any systematic trend as for example less material at the edges or very similar values at points of equal distance from the center of the target. As expected from the mass measurements,  $^{237}\text{Np}$  is the thinnest since the mass of this target is slightly bigger than the mass of  $^{235}\text{U}$  and smaller than the mass of both  $^{238}\text{U}$  targets and is distributed in a larger surface.

Furthermore, the homogeneity of the samples was examined by measuring the alpha tracks at different points of the surface with use of CR-39 plastic track detectors. The detectors were placed on top of the samples for a few seconds to a few hours, depending on the activity of the sample, in order to achieve a surface tracks concentration of at least 200 tracks/ $\text{mm}^2$ . The detectors were etched in a 6 N aqueous NaOH solution, maintained at 75°C in a water bath with a temperature control better than 1°C. Then a number of images of the detectors surfaces were captured with the use of a microscope - video camera - frame grabber - computer recording arrangement. In the present work, images were captured every 5 mm and were automatically analyzed using the TRIAC II software to count the number of tracks per  $5 \times 5 \text{ mm}^2$  and histograms like the one in Fig. 3 were obtained.

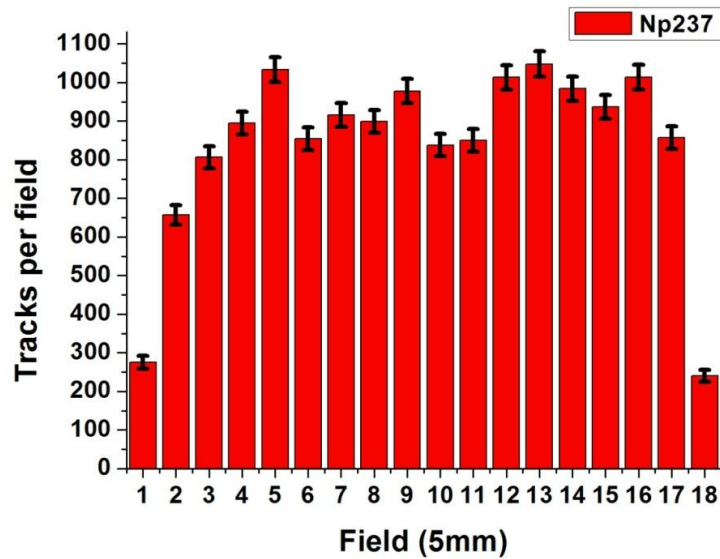


Fig. 3. A histogram of the number of alpha tracks recorded from the surface of the  $^{237}\text{Np}$  target. In order to reconstruct such histograms, images were captured every 5 mm and the number of tracks was recorded every  $5 \times 5 \text{ mm}^2$ .

The analysis gave consistent results with the RBS technique, excluding the edges. The alpha track counting showed less material at the edges, while this was not the case for the results from the RBS technique. This can be attributed to edge effects in the detection of the alpha tracks, since the CR39 detectors and the targets were of similar area.

#### 4 Conclusions

The measurement of the mass of actinide targets used for fission cross section measurements was performed via alpha spectroscopy and the analysis gave high accuracy results. The examination of the homogeneity of the targets was performed via the Rutherford Backscattering Spectroscopy and the measurement of the alpha tracks from the surface with CR-39 plastic detectors and the two methods gave consistent results. The results of the present work will be used for the extraction of the cross section value of the  $^{237}\text{Np}(n,f)$  reaction at various incident neutron energies.

## 5 Acknowledgements

This research has been co-financed by the European Union (European Social Fund - ESF) and Greek national funds through the Operational Program "Education and Lifelong Learning" of the National Strategic Reference Framework (NSRF) - Research Funding Program: Heracleitus II. Investing in knowledge society through the European Social Fund.

## References

- [1] R. B. Gardner, K. Verghese, H. M. Lee, Nucl. Instrum. Methods **176**, (1980) 615-617.
- [2] MCNPX, Version 2.5.0, LA-CP-05-0369 (Los Alamos National Laboratory, April 2005).
- [3] D. Sokaras, E. Bistekos, L. Georgiou, J. Salomon, M. Bogovac, E. A.-Siotis, V. Paschalis, I. Aslani, S. Karabagia, A. Lagoyannis, S. Harissopulos, V. Kantarelou, A.-G. Karydas, Nucl. Instr. Meth. B **269** (2011) 519-527.
- [4] M. Mayer in: J. L. Duggan, I. L. Morgan (Eds.), Proceedings of the 15th CAARI, AIP Conference Proceedings, **475** (1999) 541.
- [5] J. F. Ziegler, J. P. Biersack, U. Littmark, *The stopping and range of ions in solids* (Pergamon Press, New York 1985).